FUDMA Journal of Engineering and Technology
ISSN: 3092-9385
https://sites.google.com/fudutsinma.edu.ng/fjet
Volume 1, Issue 2, 2025, 1-18

Performance Evaluation of Climate Products with Validation Using Bootstrapping and Climate Extremes in the Hadejia-Jama'are River Basin, Nigeria

Idris M. WADA[1*], Abba IBRAHIM[2], Genesis ISHAYA[3]

[1*,3]Department of Agricultural Engineering, Faculty of Engineering, Federal University, Wukari, Nigeria
[2]Department of Agricultural and Environmental Engineering, Faculty of Engineering, Bayero University, Kano, Nigeria

[1*]wada@fuwukari.edu.ng, [2]aibrahim.age@buk.edu.ng, [3]genesisishaya14@gmail.com

Abstract

The increasing availability of satellite, reanalysis, and gauge-based Climate Products (CPs) has significantly advanced hydroclimatic research, particularly in data-scarce regions. Despite their usefulness, these CPs often carry substantial uncertainties, necessitating thorough evaluation before use in regional or basin-level studies. This study assesses the performance of nine precipitation and four temperature gridded datasets over the Hadejia-Jama'are River Basin (HJRB), Nigeria, using observational data from Kano, Jigawa, and Bauchi for the period 1990–2015. Daily and monthly precipitation (Pr), maximum temperature (Tmax), and minimum temperature (Tmin) temperature records were evaluated using Kling-Gupta Efficiency (KGE), Normalized Root Mean Square Error (NRMSE), Pearson correlation (r), Percentage Bias (PBIAS), and Mean Difference (MD). The fifth generation of the European Centre for Medium-Range Weather Forecasts (ERA5) dataset demonstrated superior performance in mean annual assessment for both Tmin and Tmax with minor underestimation. Tmax biases ranged from 2.2% to 3.5% and Tmin from 0.3% to 2.1%. Climate Forecast System Reanalysis (CFSR) had the weakest performance among the temperature products. The Climate Hazards Group InfraRed Precipitation with Station data (CHIRPS) outperformed other precipitation products, with modest underestimations of 3.5% (Kano), 9% (Bauchi), and 12% (Jigawa), while Climate Prediction Center (CPC) showed the poorest alignment with observed data. Monthly statistical evaluations yielded stronger statistical performance than daily analyses, especially for temperature datasets. For precipitation, correlation coefficients exceeded 0.5 across all models at daily resolution, with CHIRPS showing the highest values. Overall model ranking using Compromise Programming Index (CPI) and Multi-Criteria Group Decision-Making Method (MCGDM) confirmed ERA5 (for Tmax and Tmin) and CHIRPS (for precipitation) as the most reliable products. Further validation using climate extremes and bootstrapped uncertainty analysis showed that the ratio of modeled to observed extremes consistently exceeded 0.5, indicating suitability for hydrological applications. The bootstrapped 95% uncertainty bands were narrow, reflecting low uncertainty in the selected CPs. ERA5 and CHIRPS emerged as the most robust datasets for hydroclimatic studies in the Hadejia-Jama'are River Basin.

Keywords: *Climate Products, Compromise Programming, Multi-Criteria Group Decision Making, Hadejia-Jama'are River basin, Statistical evaluation, Climate extremes.*

1.0 Introduction

Climate products (CPs) serve as critical tools in providing historical climatic conditions, guiding policy decisions, and implementing adaptation and mitigation strategies[1, 2]. However, the efficacy of these models is conditional upon the availability and quality of observational data against which they can be validated and refined. This becomes a significant challenge in data-scarce regions, where limited ground-based observations hinder the comprehensive evaluation and improvement of climate models[2]. The Hadejia-Jama'are River Basin (HJRB) in Northern Nigeria exemplifies such a region, where data paucity undermines the ability to conduct robust climate studies[3]. In data scarce regions, the accuracy of hydrometeorological research is greatly affected by the temporal and spatial availability of gauged data, as well as the quality of these observations[4]. However, climate data from ground-based meteorological stations often lack consistency and reliability due to factors such as a limited number of stations, uneven geographical coverage, and susceptibility to both human and environmental disturbances[5]. For example, The World Meteorological Organization (WMO) recommends gauge density based on the terrain being monitored. The recommended density for rain gauge in flat areas ranges from 600-900 km^2/gauge, while 100-250 km^2/gauge is recommended for rugged region.

Given the scarcity of observational data in the Hadejia-Jama'are River Basin, CPs such as satellite, reanalysis, and gauge-based climate models emerge as invaluable assets. These products, each with its unique methodological approach and source of data input, offer alternative avenues to obtain climate-related data[6, 7]. In light of these scarcity, gridded climatic datasets at regional and global levels have become valuable alternative sources of climate information[4]. This shift is largely driven by advancements in remote sensing and data assimilation technologies[8].

Received: 28/06/2025; Revised: 03/07/2025; Accepted: 03/07/2025; Published: 08/08/2025

Nevertheless, the reliability of these datasets in replicating ground-based observations and supporting hydrological modeling varies significantly across different regions and river basins. Although CPs offer extensive spatial and temporal coverage and are unaffected by local weather conditions or wind, they often exhibit biases and regional inconsistencies, necessitating evaluation against ground-based observations.

Given the vast number of available CPs, the choice of product significantly influences decision-making in critical areas such as water management and planning[2]. Numerous studies have evaluated gridded precipitation and temperature data against gauge data to determine their accuracy and reliability[e.g. 9, 10-13]. The conclusions of these studies vary depending on the locations, spatial extent, and time steps of the analyses[e.g. 9, 11, 13-15]. Most studies have assessed accuracy using observed meteorological data[e.g. 16, 17-19] or gauge-adjusted radar fields[e.g. 20, 21]. Many studies have quantified the performance of different precipitation datasets using hydrological modeling by comparing simulated and observed streamflow values[e.g., 22, 23-25] or soil moisture comparisons[e.g., 26, 27, 28]. Some researchers have used extreme analysis as a means of evaluation[29]. Differences in spatio-temporal patterns in precipitation and temperature accuracy have been found among the datasets, even those using the same data sources. Despite these uncertainties, gridded products have proven beneficial in various watersheds around the world. For instance, CHIRPS precipitation data have shown high correlation with minimal bias in East Africa, Egypt, and Iran[30-32]. The Tropical Rainfall Measuring Mission (TRMM) 3B42 dataset, evaluated in numerous studies[e.g., 33, 34] in China, and has been recommended for hydrological modeling in regions like the upper Indus Basin of Pakistan[35]. The Precipitation Estimation from Remotely Sensed Information using Artificial Neural Networks - Climate Data Record (PERSIANN-CDR) performed well in eastern China [36], and showed good correlation in West Africa[37].

Several studies have evaluated the performance of gridded climate datasets across Nigeria, revealing significant spatial and temporal variations in their accuracy and suitability for climate and hydrological applications. For instance, [38] assessed monthly precipitation using three gridded datasets and reported that all products performed poorly in northern stations during the dry season but showed good agreement with observations across the country during the wet season. Among the datasets evaluated, the Global Precipitation Climatology Centre (GPCC) product exhibited the best overall performance. In a similar study across Nigeria, [39] identified GPCC and the Global Precipitation Climatology Project (GPCP) as the top-performing datasets for precipitation, although their effectiveness varied across different eco-climatic zones. Similarly, [40] ranked the Climate Research Unit (CRU) model as the most reliable product for rainfall, minimum and maximum temperature. Conversely, [41] identified CHIRPS with highest agreement against observed data in all climatic zones of Nigeria, accurately reflecting local rainfall characteristics. This further reflects the inconsistency in dataset performance depending on the evaluation method and region of interest. This regional variation highlights the importance of selecting climate products that are tailored to specific temporal and homogenous geographical contexts to enhance the reliability of climate research and resource management, especially in data-scarce regions. Despite these national-level assessments, limited studies have focused specifically on the HJRB, a critical hydrological zone in northern Nigeria characterized by high climate variability, sparse observation networks, and increasing water resource demands. Existing CPs such as CHIRPS, GPCC, GPCP, CRU, CFSR, and ERA5 have been widely used in the region, yet their comparative performance and associated uncertainties within HJRB remain underexplored. This presents a significant gap in localized model selection necessary for improving hydrological simulations, climate impact assessments, and water resources planning in the basin.

Therefore, to obtain more generally acceptable gridded products, it is essential to thoroughly evaluate these datasets in terms of pattern reproduction, magnitude, variability, extremes, and uncertainties contained in the variables. In this study, for the selection of temperature variables, we hinged on their capability to accurately replicate both maximum and minimum temperatures, as both extremes are essential for comprehensive temperature-related studies. For Precipitation, careful considerations were made to ensure the selected models adequately reflect the precipitation patterns and extremes of the region under study. To this end, this study adopts a robust multi-step approach that integrates compromise programming and a multi-criteria group decision-making method (MCGDM) to systematically evaluate and rank three reanalysis, two satellite-based, and two gauge-based products for precipitation, along with three reanalysis and one gauge-based model for temperature. The specific objectives of the study are to: (1) Evaluate the performance of selected precipitation and temperature climate products (CPs) against observed data using statistical and correlation metrics at daily and monthly timescales. (2) Rank the performance of the CPs using compromise programming and synthesize the rankings across stations through a multi-criteria group decision-making method (MCGDM) approach to identify the most representative products. (3) Validate the selected CPs through climate extremes analysis and quantify their associated uncertainties using a non-parametric bootstrapping technique with 95% uncertainty bands.

2.0 Study area and data

2.1 The Hadejia-Jama'are River Basin

Received: 28/06/2025; Revised: 03/07/2025; Accepted: 03/07/2025; Published: 08/08/2025

The Hadejia-Jama'are River Basin (HJRB), situated in Northern Nigeria (Figure 1), is a critical inter-state transboundary basin that spans across Kano, Jigawa, Bauchi, and Yobe states. It covers a catchment area of approximately 48,891 square kilometers; the basin is geographically defined by longitudes 7.32 to 11.05 and latitudes 9.84 to 12.96 degrees. It is characterized by a semi-arid to arid climate, the region experiences significant climatic challenges that influence its hydrology and water resource management. Central to the basin's hydrological framework are the Tiga and Challawa Dams (Figure 1), which play pivotal roles in controlling the flow of the River Kano and subsequently the River Hadejia.

The region's climate is predominantly hot and dry, marked by distinct wet and dry seasons. The wet season spans from June to September, offering a relief from the intense dry heat, while the dry season extends from November to May, during which temperatures decline substantially during the harmattan (December through February) and then soar above 40 degrees Celsius in May. The land use in the basin is primarily dominated by extensive croplands for both irrigation and rainfed agriculture, with significant areas dedicated to wetlands downstream, scrublands, and minimal forest areas. The climatic conditions and land use practices in the HJRB present unique challenges and opportunities for water resource management.

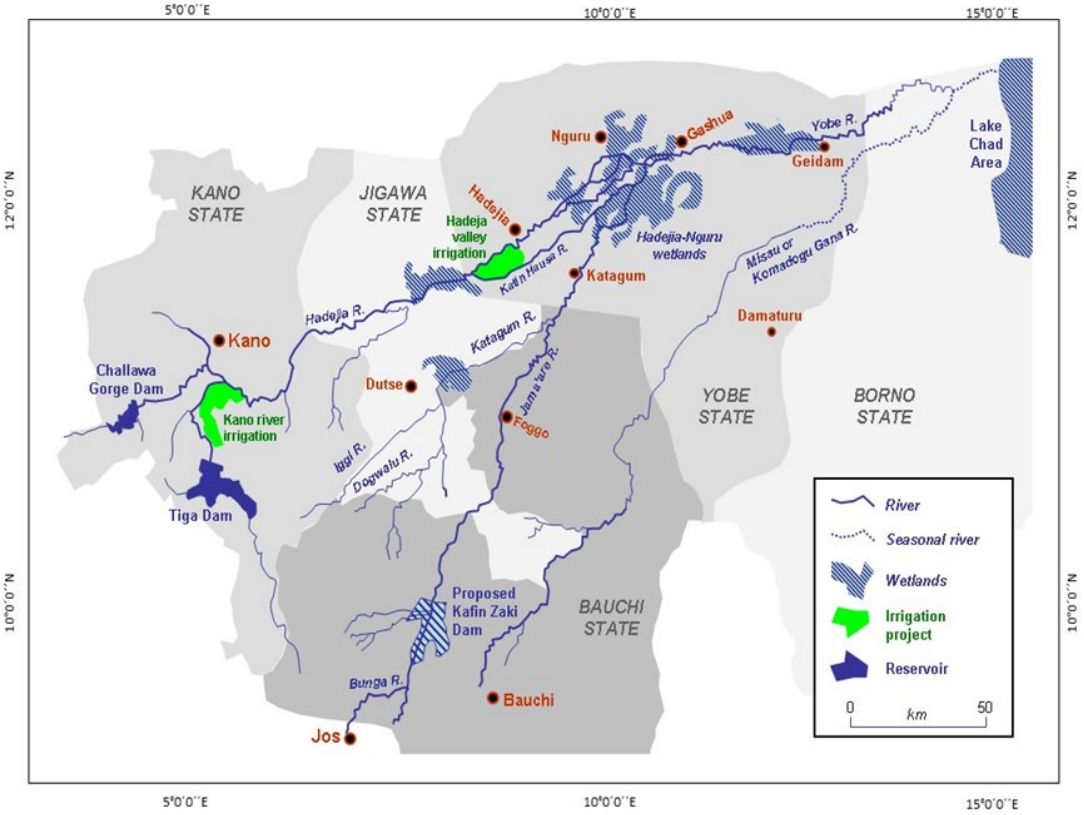

Figure 1: Study area comprising of irrigation projects, reservoirs, wetlands, and river networks in Hadejia-Jama'are River Basin. The upstream consist of Tiga and Challawa Dams, and the rivers discharges into Lake Chat area. (Source: Wikipedia)

2.2 Dataset

For the comprehensive evaluation of CPs in the Hadejia-Jama'are River Basin, this study utilized daily precipitation data along with daily minimum and maximum temperature records obtained from three strategically chosen observational stations located in Kano, Jigawa, and Bauchi states. These stations were specifically selected based on the continuous, quality, and reliable observational data available for the period spanning from 1990 to 2015, courtesy of the Nigerian Meteorological Agency (NiMet). The geographical distribution of these stations across different climate zones within the study area ensures a representative sampling of the region's climatic variability, thus providing a robust basis for the evaluation of climate models.

The climate models employed in this study encompass a diverse array of sources, including reanalysis, satellite, and gauge-based data, to ensure a comprehensive evaluation of their performance in replicating observed climatic conditions within the basin. The reanalysis models include the fifth generation (ERA5) of the European Centre for Medium-Range Weather Forecasts (ECMWF) reanalysis for the global climate and weather for the past few decades [42], the Modern-Era Retrospective analysis for Research and Applications (MERRA-2) version 2, provided by NASA's Global Modeling and Assimilation Office[43], and the Climate Forecast System Reanalysis (CFSR) by the National Centers for Environmental Prediction[44]. For satellite-derived precipitation estimates,

Received: 28/06/2025; Revised: 03/07/2025; Accepted: 03/07/2025; Published: 08/08/2025

this study utilized the Precipitation Estimation from Remotely Sensed Information using Artificial Neural Networks (PERSIANN), developed by the Center for Hydrometeorology and Remote Sensing at the University of California, Irvine[36], and the Climate Hazards Group InfraRed Precipitation with Station data (CHIRPS), a quasi-global rainfall dataset designed to blend satellite imagery with in-situ station data[45]. The gauge-based models included in this study are the Global Precipitation Climatology Centre (GPCC), offering globally gridded precipitation analyses from rain gauge data[46], and the Climate Prediction Center (CPC) Global precipitation and temperature data, which provides global analyses from gauge observations. These climate models were selected based on the criteria that they consist of temporal resolution of daily time series and spans from 1990 to present (Table 1).

Table 1: Summary of Climate Products

Data set	Variable	Spatial resolution	Frequency	Coverage	Temporal coverage	Source	Reference
Gauge-base Products							
GPCC	Pr	1.0° × 1.0°	Daily	Global land	1980-2022	GPCC	[47]
CPC	Pr, Tm	0.5° × 0.5°	Daily	Global land	1979-present	CPC	[48]
Satellite-Related Products							
PERSIANN-CDR	Pr	0.25°	Daily	Global land	1982-present	NOAA	[49]
CHIRPS	Pr	0.05°	Daily	Global land	1981-present		[50]
Reanalysis Products							
ERA5	Pr, Tm	0.25° × 0.25°	Daily	Global land	1940-present	ECMWF	[51]
MERRA2	Pr, Tm	0.25° × 0.25°	Daily	Global land	1980-present	NASA	[52]
CFSR	Pr, Tm	38 km	Daily	Global land	1979-present	NOAA	[53]

These data sources were downloaded from the Climate Data Engine and processed using the R programming software to ensure consistency and accuracy in the evaluation process.

2.3 Research Method

The methodology precisely integrates model selection and evaluation to find the best performing model in representing the precipitation and temperature condition in the HJRB, and quantified the uncertainties in the best model. The principle behind the methodology is based on the evaluation of climate data products to determine which best represents the local climate conditions of the study area. The comprehensive procedure is succinctly illustrated in the flowchart provided in (Figure 2).

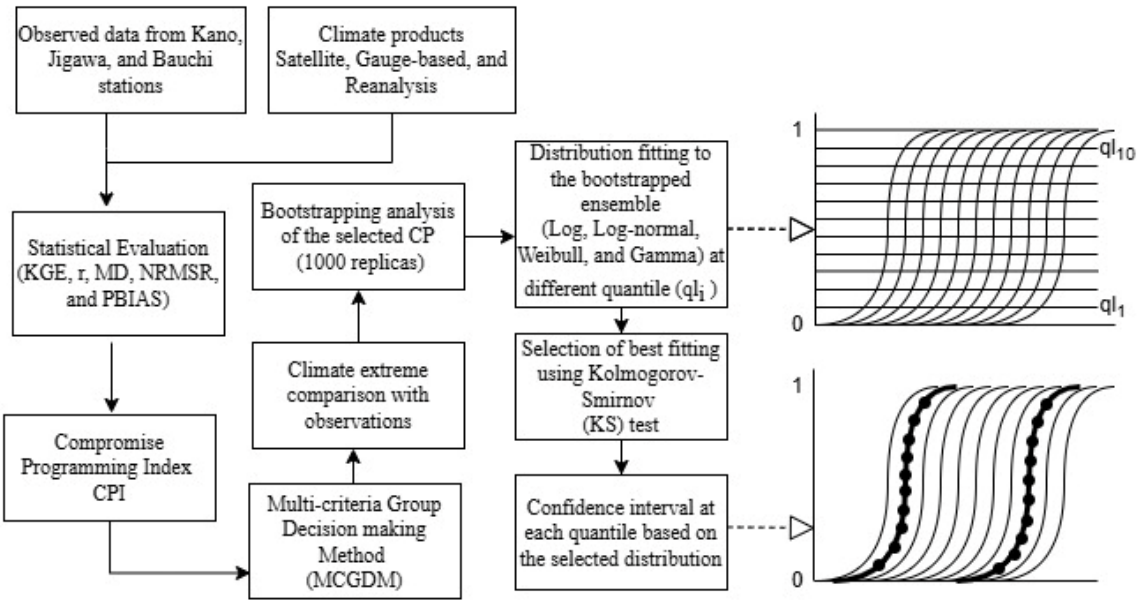

Figure 2: The methodological framework

2.4 Performance Evaluation

Received: 28/06/2025; Revised: 03/07/2025; Accepted: 03/07/2025; Published: 08/08/2025

Temperature and precipitation products were evaluated using R software for statistical evaluation and analysis. The evaluation employed five statistical metrics (Table 2); the normalized root mean square error (NRMSE), percentage of bias (PBIAS), Kling-Gupta Efficiency (KGE), modified index of agreement (MD), and the Pearson product-moment correlation coefficient (r). These metrics collectively assess different aspects of model performance, including pattern reproduction, variability, and average conditions, thus providing a holistic evaluation of the CPs. The ideal values, expressions, and possible ranges of these metrics are systematically tabulated in (Table 2).

Table 2: The statistical indices used for the assessment of climate model temperature and precipitation

Metric name	Index	Range	Optimal value
KGE (Kling-Gupta Efficiency)	$KGE = 1 - \sqrt{(r-1)^2 + (\beta-1)^2 + (\gamma-1)^2}$	-∞ to 1	1
PBIAS (Percentage Bias)	PBI $AS = \frac{\sum_{i=1}^{n} (P_i - O_i)}{\sum_{i=1}^{n} O_i} \times 100$	-∞ to +∞	%
r (Pearson Correlation Coefficient)	$r = \frac{\sum_{i=1}^{n} (O_i - \bar{O})(P_i - \bar{P})}{\sqrt{\sum_{i=1}^{n} (O_i - \bar{O})^2 \sum_{i=1}^{n} (P_i - \bar{P})^2}}$	-1 to 1	1
NRMSE (Normalized Root Mean Square Error)	$NRMSE = \frac{\sqrt{\frac{1}{n}\sum_{i=1}^{n} (O_i - P_i)^2}}{\bar{O}}$	0 to +∞	0
MD (Modified Index of Agreement)	$MD = 1 - \frac{\sum_{i=1}^{n} \lvert P_i - O_i \rvert}{\sum_{i=1}^{n} \lvert P_i - \bar{O} \rvert + \lvert O_i - \bar{O} \rvert}$	0 to 1	1

where, O_i and P_i are the observed and model value of the variables respectively; $\bar{O}$ is the mean of observed values; $\bar{P}$ is the mean of model values; In KGE, r is the Pearson correlation coefficient, β is the bias ratio (mean of simulated values/mean of observed values), and $\gamma$is the variability ratio (coefficient of variation of simulated values/coefficient of variation of observed values).

2.5 Compromise Programming and Multi-Criteria Group Decision Making Method

Compromise Programming (CP) and Multi-Criteria Group Decision Making method (MCGDM) are both pivotal methodologies within the field of operational research, especially when dealing with complex decision-making scenarios that involve multiple criteria or objectives. Compromise Programming (CP) was utilized to integrate the outcomes from the statistical indices into a single metric, NRMSE and PBIAS metrics were normalized to ensure consistency in evaluation. Lower CPI show good performance, indicating lower distance from the ideal point. The compromise programming index (CPI) is presented in Equation 1, vis;

$$CPI = (\sum_{i=1}^{n} |z_i - r_i|^p)^{\frac{1}{p}} \quad (1)$$

where, *CPI* is the Compromise Programming Index, *n* is the number of evaluation metrics, *zi* is the normalized value of the model for metric *i*, *ri* is the normalized ideal value of the metric *i*, while *p* is the power parameter, in which 1 represents linear distance and 2 represents squared Euclidean distance (linear distance was adopted herein). This approach facilitates the identification of the most representative climate model by estimating its proximity to an ideal point, where the ideal point represents the optimal values of the evaluation metrics. CP effectively ranks the performance of different models at each station. However, addressing the challenge of selecting an overall model for the entire basin, a Multi-Criteria Group Decision-Making Method (MCGDM) was proposed. It is particularly useful when decisions need to be made collaboratively by groups with potentially diverse preferences and perspectives. Each climate model was evaluated at different stations, and a collective decision was made regarding the overall ranking of the models. This was achieved by aggregating the rankings from each station, taking into account the relative importance or weight at each station during evaluation. Weights were derived in such a way that the inverses of each model were ranked at every station and then summed. The higher weight indicates better product performance. The method was applied to both daily and monthly time-step and aggregated the ranking. The MCGDM was calculated via Equation 2, viz,

$$W_i^{(z)} = \sum_{j=1}^{m} \frac{1}{R_{ij}^{(z)}} \quad (2)$$

where, $R_{ij}^{(z)}$ is the rank of the model *i* at station *j* for variable *z* (daily precipitation or temperature), *m* is the total number of observed stations, while $W_i^{(z)}$ is the normalized aggregated inverse rank.

Received: 28/06/2025; Revised: 03/07/2025; Accepted: 03/07/2025; Published: 08/08/2025

2.6 Climate Extremes Indices

In this study, we employed a nonparametric approach to analyze extreme rainfall events within the HJRB by calculating five distinct indices (referenced in Table 3). These indices are designed to calculate the extreme rainfall climatology relevant to the area under investigation. Additionally, we evaluated two indices related to temperature extremes.

For precipitation extremes, our methodology involved the application of skewness, the relative frequency of days with precipitation equal to or exceeding 10mm, the 98th percentile of days with precipitation (≥1mm), the mean precipitation on wet days (defined as days with ≥1mm precipitation, also known as the Simple Day Intensity Index, SDII), and the relative amplitude of the daily annual precipitation cycle expressed as a percentage relative to the mean. These indices are instrumental in characterizing the magnitude and frequency of extreme precipitation events in the study area[54].

Table 3: Extreme precipitation and temperature indices used in this study

Category	Index	Description
Magnitude	SDII	Simple Day Intensity Index (Mean wet day ≥1mm precipitation
	P98thwet	98th percentile of wet (>=1 mm) days
	WarmSpellP90	90th percentile of the annual warm (> 90th percentile) spell maxima
	Skewness	Skewness
	WarmAnnualMaxSpell	Median of the annual warm (> 90th percentile) spell maxima
	ColdAnnualMaxSpell	Median of the annual cold (< 10th percentile) spell maxima
	AnnualCycleRelAmp	Relative amplitude of the daily annual cycle (%, relative to the mean)
Freqeuncy	R10	Relative frequency of days with precip >= 10mm
	ColdSpellP90	90th percentile of the cold (< 10th percentile) Spell Length Distribution

For temperature extremes, we calculated the 90th percentile of the annual maximum temperatures that exceed the 90th percentile threshold, as well as the median of these annual warm spell maxima for Tmax, while For Tmin, we analyzed the 90th percentile of the cold spell percentile and the median of the annual cold spell maxima.

The chosen indices are based on both absolute values and percentile-based thresholds, allowing for a comprehensive evaluation of climate products. Notably, these indices are included in the Expert Team on Climate Change Detection and Indices (ETCCDI) (http://etccdi.pacificclimate.org/indices_def.shtml), and[55, 56]. The ETCCDI indices are globally recognized and have been extensively applied in studies focusing on the detection, attribution, and projection of climate change phenomena. The ration of the climate products was calculated with respect to the observed datasets yielding the variations in the climate products.

2.7 Uncertainty Analysis

Dataset, such as precipitation and temperature, are often subjected to various sources of uncertainty, including measurement errors, instrument limitations, and spatial/temporal variability. Understanding and quantifying these uncertainties are crucial for reliable water resource assessments and decision-making[57]. The uncertainty quantification commenced with the aggregation of daily precipitation data into monthly totals for each year, focusing solely on the months from June to September for precipitation to capture the rainy season dynamics, and the entire year for temperature. The aggregated data were then fitted to four distinct distributions including Normal, Log-Normal, Gamma, and Weibull. The goodness of fit for each distribution was assessed using the nonparametric Kolmogorov-Smirnov (KS) test, with the distribution exhibiting the lowest KS score selected as the best fit. Bootstrapping, Efron [58] was employed to generate 1000 replicas with replacement of the monthly data for each station. These replicas were then used to construct Cumulative Distribution Functions (CDFs) for better representation of the results[57]. The CDF, derived from all replicas, served as the foundation for constructing quantile lines (ql) ranging from the 10th to the 90th percentile on the probability axis (y-axis). Defining the distribution of the precipitation and temperature replicas at each quantile would describe the dispersion and probability of occurrence of different replica. The best-fit distribution was then used to obtain the confidence interval of the CDF replicas at each quantile line (Figure 2). The 95% confidence intervals were calculated at each line across all replicas, creating an upper and lower bound of the uncertainty. Connecting these points for all the quantiles reveals the uncertainty band. The overall CDF from the bootstrapped replicas, complemented by the 95% confidence interval bounds, encapsulates the uncertainty in the estimations and provides a vivid representation of the selected model predictive reliability. This careful approach to model evaluation and uncertainty analysis, supported by robust statistical methods and innovative decision-making frameworks, constitutes the core of the research methodology employed in this study, ensuring a comprehensive and reliable assessment of climate model performance in the HJRB.

Received: 28/06/2025; Revised: 03/07/2025; Accepted: 03/07/2025; Published: 08/08/2025

3.0 Results and discussion

3.1 Performance Assessment of Temperature and Precipitation

The detailed performance assessment calculated from their annual means of temperature and precipitation variables from 1990 to 2015 by the CPs reveals varying insights into their predictive capabilities. The analysis showed the mean annual changes in Tmax and Tmin, and the mean annual precipitation (Pr) sum over the study period, providing insight into the ability of the CPs to replicate observed trends. For Tmax (Table 4), the ERA5 reanalysis model demonstrated the best performance among the evaluated products, although with a consistent underestimation across the stations; 2.2% in Kano, 2.5% in Jigawa, and 3.5% in Bauchi. This indicates a relatively close approximation to the observed temperature trends, though with a slight tendency towards cooler temperatures. In contrast, the CFSR model exhibited the least accurate performance, with significant overestimations of 13% in Kano, 8.5% in Jigawa, and 6.8% in Bauchi. Such discrepancies suggest a systematic bias in the CFSR model towards warmer temperatures. The analysis of Tmin (Table 4) revealed that ERA5 outperformed other products, presenting minor underestimations of 1.4% in Kano, 0.3% in Jigawa, and 2.1% in Bauchi. These findings indicate a high degree of accuracy in capturing the cooler temperature ranges. Conversely, the CFSR model again showed the least favorable performance, with substantial underestimations of 9.5% in Kano, 7.6% in Jigawa, and 10.4% in Bauchi. Such underestimations by the CFSR model highlight its limitations in accurately capturing the minimum temperature trends across the stations.

The assessment of precipitation (Pr) performance (Table 4) by the climate models revealed significant variability in their accuracy. The CHIRPS dataset showed the best agreement in simulating precipitation patterns, closely aligning with observed data. For the Kano and Bauchi stations, CHIRPS exhibited underestimations of 3.5% and 9%, respectively, suggesting a modest deviation from observed precipitation levels. Interestingly, at the Jigawa station, CHIRPS showed an overestimation of 12.1%, indicating a tendency to predict higher precipitation levels than observed. On the other end, the CPC model displayed the least accurate precipitation predictions. It significantly underestimated precipitation in Kano and Bauchi by 21.2% and 28.7%, respectively, pointing to a pronounced dry bias in the model. Conversely, at the Jigawa station, the CPC model overestimated precipitation by 19.6%, revealing an inconsistency in its performance across different locations.

Table 4: Mean annual performance of Tmax, Tmin and Pr with respect to observation

Variable	Climate Products	Stations		
		Kano	Jigawa	Bauchi
Tmax	CPC	-2.8	-2.8	-6.7
	MERRA-2	-2.5	-2.9	-4.4
	CFSR	13.0	8.5	6.8
	ERA5	-2.2	-2.5	-3.5
Tmin	CPC	-1.6	-2.3	-2.3
	MERRA-2	-4.9	-3.7	-5.2
	CFSR	-9.5	-7.6	-10.4
	ERA5	-1.4	-0.3	-2.1
Pr	CHIRPS	-3.5	12.1	-9.0
	CPC	-21.2	19.6	-28.7
	CFSR	-27.8	33.0	-28.5
	ERA5	-20.7	-16.3	-15.4
	GPCC	-10.7	13.9	-10.9
	MERRA-2	-7.3	27.1	-28.3
	PERSIANN-CDR	-11.5	32.7	-14.3

3.2 Statistical Evaluation for Temperature and Precipitation

The assessment of CPs performances skills towards observed Tmax, Tmin, and Pr involving suits of statistical metrics (NRMSE, MD, KGE, PBIAS, and r) were calculated at daily and monthly time steps across three station locations. The normalization of NRMSE and PBIAS to a 0-1 scale facilitates an intuitive interpretation of the results, where values closer to 0 indicate better model performance. For Tmax, KGE demonstrated good result across all stations, with values exceeding 0.5 at both daily and monthly time steps. The monthly time step, in particular, showed exceptional performance with KGE values often surpassing 0.8, highlighting the products

Received: 28/06/2025; Revised: 03/07/2025; Accepted: 03/07/2025; Published: 08/08/2025

accuracy in capturing Tmax variability on a broader temporal scale. The ERA5 model consistently emerged as the top performer in this metric. The metric r, indicated strong correlations exceeding 0.5 for all products at both time steps, with the ERA5 model achieving the highest correlation values, especially at the monthly time step, reflecting its superior capability in mirroring the observed Tmax trends. NRMSE Revealed lower errors for all models at the monthly time step compared to the daily, with values approaching 0 indicating minimal deviation from observed data. The monthly aggregation appears to smooth out daily variability, leading to reduced error margins. In MD, Except for the ERA5 model, other models exhibited weaker values, indicating a less satisfactory agreement with observed data, especially on a daily scale. The CFSR model displayed negative MD values across all stations and time steps, underscoring its challenges in accurately capturing Tmax dynamics. PBIAS highlighted the CFSR model as having the highest bias across stations, suggesting a systematic deviation from observed Tmax values. Conversely, the ERA5 model maintained the lowest bias, affirming its robustness in Tmax simulation.

KGE and r metrics showcased commendable results in Tmin, similar to Tmax, with even higher values observed at the monthly time step. The ERA5 model stood out with the highest metric values, highlighting its proficiency in capturing Tmin variations. Across the CPs, NRMSE values were closer to 0, indicating minimal error, with MERRA-2 and ERA5 showing particularly strong performance at the daily time step. This trend of reduced error persisted and improved at the monthly time step.

For Pr, during the daily time Step, the models generally exhibited poorer performance, with the notable exception of r, where all models achieved values greater than 0.5, indicating a reasonable degree of correlation with observed precipitation. CHIRPS distinguished itself with the highest r value, suggesting its relative effectiveness in daily precipitation estimation. Monthly time Step displayed improved model performance in terms of KGE and r, reflecting better alignment with observed precipitation patterns when analyzed on a broader temporal scale. However, NRMSE values diverged further from 0, signifying increased error in monthly precipitation estimates. Conversely, daily time step evaluations showed less error. PBIAS indicated a reversal in bias trends, with models exhibiting more significant bias at the daily time step compared to the monthly. This suggests that while models may capture the general precipitation trends on a monthly basis, they struggle with day-to-day variability.

The statistical metrics employed reveal that models generally perform better at monthly time steps, particularly for temperature variables, as evidenced by higher KGE and r values and lower NRMSE. Precipitation products have a challenge, particularly at daily time steps, though certain models like CHIRPS show promise. The ERA5 model consistently performed better across temperature variables highlighting its utility in climate studies, while for CFSR, significant biases and errors indicate areas for the product improvement. These insights are crucial for understanding model strengths and limitations, guiding model selection and application in climate research and water resource management.

3.3 Ranking of Temperature and Precipitation

The application of Compromise Programming (CP) in this study aimed to aggregate the performance metrics of various climate models into a single Compromise Programming Index (CPI), facilitating a comprehensive comparison of model performances across three distinct stations. The CPI serves as a unified measure of model performance, with lower values indicating closer alignment with the ideal model performance and, consequently, better overall capability. Figure 3 presents the CPI results in the form of a heatmap, offering a visually intuitive representation of the CPs performances across the Kano, Jigawa, and Bauchi stations. The color gradient in the heatmap, transitioning from deep blue to green to yellow, intuitively conveys the performance spectrum of the evaluated climate models. Deep blue sorts signify models with superior performance, denoted by lower CPI values, reflecting their closer proximity to the ideal performance criteria across the evaluated metrics. Conversely, cells colored in shades of yellow indicate models with higher CPI values, signifying a larger deviation from the ideal and, thus, lesser capability in replicating observed climate variables.

Received: 28/06/2025; Revised: 03/07/2025; Accepted: 03/07/2025; Published: 08/08/2025

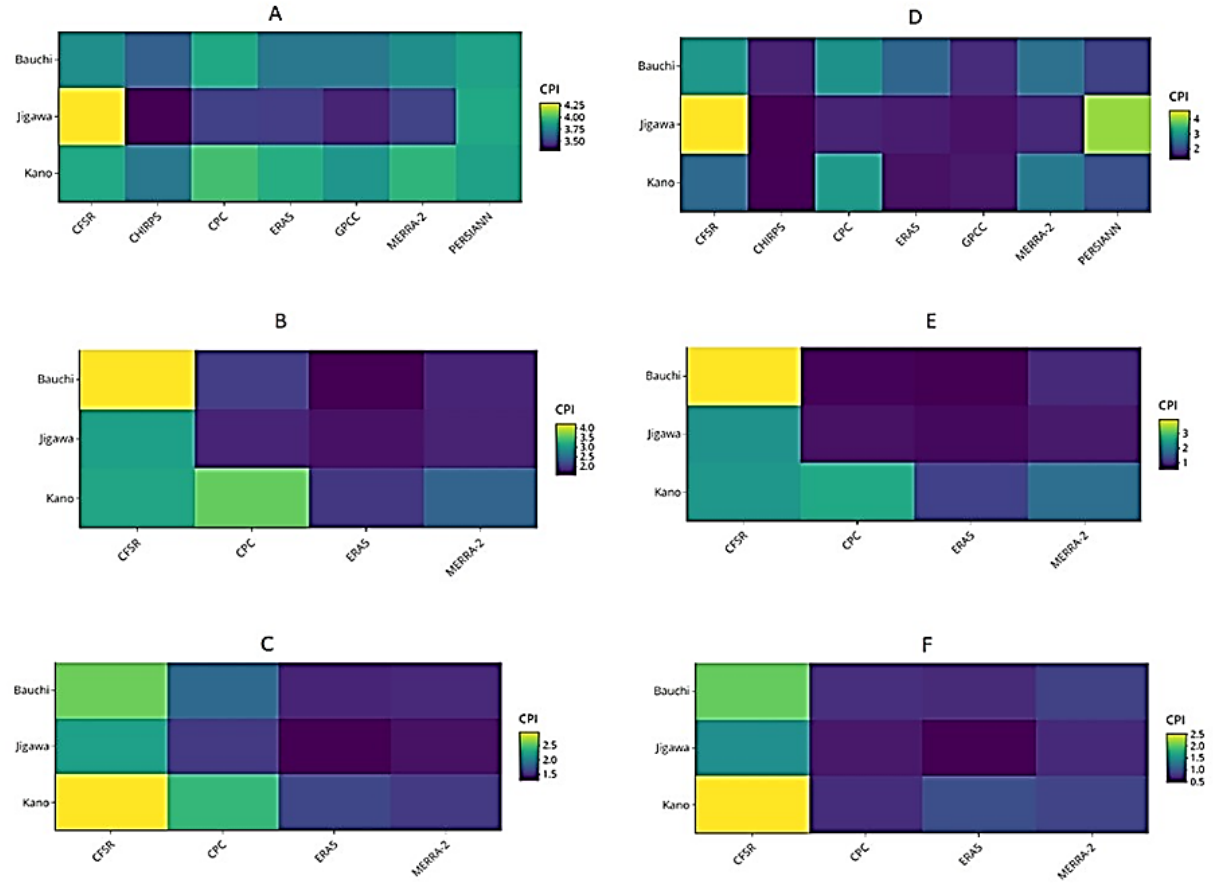

Figure 3: Heatmap of CPI for all Climate Products and Stations used in this study. Daily Pr (A), Daily Tmax (B), daily Tmin (C), monthly Pr (D), monthly Tmax (E), and monthly Tmin (F)

The CPI heatmap shows CHIRPS and ERA5 models performing better as a result of lower index values.

3.4 Multi-Criteria Group Decision Making Process

The Multi-Criteria Group Decision Making (MCGDM) approach was utilized to synthesize the ranks of various climate models across different stations, thereby enabling a rational selection of the most suitable model for representing climate variables across the entire HJRB. This methodological approach is particularly effective in aggregating individual model performances at various locations in daily and monthly time-step to deduce a consensus on the best-performing models for Tmax, Tmin, and Pr datasets. Table 5 illustrates the ranking of climate models for Tmax, Tmin, and Pr datasets, initially derived using CPI and subsequently integrated through the MCGDM process. The integration involved assigning weights to the models based on their performance ranks (1st, 2nd, and 3rd) at each station, thus reflecting their relative performance merits across the basin. Subsequently, an integrated MCGDM index was calculated for each model using equation 2, where a higher index value signifies superior performance of a CP. This index effectively combines the individual station rankings into a unified basin-wide performance metric. The overall model performance rankings process led to the following key insights for Tmax, Tmin, and Pr across the HJRB. In temperature Variables (Tmax and Tmin), the ERA5 model was identified as the top-performing product. The model was robust and consistent across the stations rendering it a reliable choice for temperature-related studies in the region. Following closely, MERRA-2 was ranked as the second-best model, indicating its commendable performance in temperature simulations.

For Pr, CHIRPS emerged as the best-performing product, highlighting its skill in capturing precipitation patterns across the basin. CHIRPS performance in simulating rainfall makes it an invaluable tool for hydrological modeling and water resource management in the region. GPCC model followed closely as the second-ranked model for precipitation, indicating its reliable performance.

Table 5: The overall ranking of the Tmax, Tmin, and Pr datasets in the HJRB, based on multicriteria group decision analysis

Variable	MODEL	MCGDM daily	MCGDM monthly	MCGDM aggregate
Tmax	ERA5	5.50	5.33	5.42
	MERRA2	3.50	2.33	2.92

Received: 28/06/2025; Revised: 03/07/2025; Accepted: 03/07/2025; Published: 08/08/2025

Variable	MODEL	MCGDM daily	MCGDM monthly	MCGDM aggregate
	CFSR	1.58	1.58	1.58
	CPC	1.92	3.25	2.58
Tmin	ERA5	2.50	2.30	2.4
	MERRA2	2.0	1.20	1.60
	CFSR	0.75	0.75	0.75
	CPC	1.0	2.0	1.50
Pr	ERA5	1.03	1.08	1.06
	MERRA2	0.53	0.57	0.55
	CFSR	0.64	0.49	0.56
	PERSSIAN	0.87	0.75	0.81
	CHIRPS	2.33	3.00	2.67
	GPCC	1.83	1.30	1.57
	CPC	0.54	0.56	0.55

The selection of CHIRPS for precipitation and ERA5 for temperature aligns with several recent studies across West Africa, which report their strong agreement with ground observations and suitability for hydrological applications. These datasets consistently outperform others in terms of accuracy, spatial coverage, and reliability, particularly at monthly timescales[41, 59-61].

3.5 Extreme Indices for the Selected Climate Products

The results obtained from the selected products (CHIRPS and ERA5) reveal significant insights into the performance of the CPs in replicating observed climatic extremes (Figure 4) in terms of both magnitude and frequency which is essential for climate change adaptation. In the analysis for magnitude, for precipitation, the CPs consistently underestimated the observed data for both the Simple Day Intensity Index (SDII) and the 98th percentile of wet days (P98thWet), with ratio values ranging between 0.56 to 0.68 and 0.64 to 0.70 in the daily timestep respectively. The relatively low ratios indicate that the CPs might not fully capture the intensity of extreme rainfall events on a daily basis. The best performance was observed at the Jigawa station, which could be due to regional climatic characteristics or station-specific factors. Using the relative amplitude index (AnnualCycleRelAmp), the CPs showed better performance in capturing the relative amplitude of the daily annual cycle, with ratio values close to 1 (0.95 to 1.0). This suggests that the model is relatively accurate in simulating the seasonal variation of rainfall, even though it underestimates the intensity of extreme events. For the monthly time scale, using the skewness, the climate product also underestimated observed data, though with somewhat better ratios (0.58 to 0.74), indicating a modest underestimation of the asymmetry in the distribution of monthly precipitation amounts. Interestingly, the CPs overestimated the monthly P98thWet at the Jigawa station, suggesting a possible over-sensitivity of the model to extreme precipitation events on a monthly scale in this region.

For Tmax, the 90th percentile of the annual warm spell maxima (WarmSpellP90) was overestimated in Jigawa (ratio of 1.1) but underestimated in Bauchi and Kano (ratios of 0.6 and 0.7, respectively). This inconsistency might be attributed to the model's varied performance across different geographical locations or its sensitivity to specific regional climatic drivers. Median Annual Warm Spell Maxima (WarmAnnualMaxSpell) indices, showed improvement across sites, with ratios ranging from 0.7 to 1.2. The overestimation in Jigawa (ratio up to 1.2) contrasts with more accurate or slightly underestimated ratios in Kano and Bauchi, stressing the differential regional performance of the CPs. A better performance was seen in the extreme monthly timestep.

For Tmin, the median of the annual cold spell maxima (ColdAnnualMaxSpell) was between the ratios ranging from 0.5 to 1.3, indicating potential limitations in their ability to capture the extremity of cold temperature spells. A better performance was observed in the Median of the annual cold (< 10th percentile) spell maxima (coldSpellP90).

In the frequency analysis, for R10 Index, the climate product slightly overestimated the frequency of days with precipitation ≥10mm (ratios ranging from 1.02 to 1.09). This suggests that while the model might underestimate the intensity of extreme precipitation events, it could be capturing their frequency somewhat more accurately. Tmin Cold Spells, the 90th percentile of the cold spell length distribution was overestimated in Jigawa (ratio of 1.15), indicating the model predicts cold spells more frequently than observed. Conversely, in Kano and Bauchi, the model underestimated these cold spells (ratios of 0.75 and 0.85, respectively), reflecting the spatial inconsistency. However, a good ratio in simulating temperature extremes was obtained.

The variability in ratio values across different indices and stations highlights the challenges in accurately simulating climate extremes due to the complex relationship of local climatic conditions, topography, and other regional factors[7]. However, for hydrological studies, the suitability of CPs especially when the ratio values of

Received: 28/06/2025; Revised: 03/07/2025; Accepted: 03/07/2025; Published: 08/08/2025

extreme indices are above 0.5, can be substantiated by several factors. These ratios indicate a moderate to high correlation between the CPs and observed data, suggesting that the CPs can indeed capture the key patterns and magnitudes of hydrological extremes, although with some underestimation or overestimation. Chiew and McMahon [62] discussed the thresholds of correlation and accuracy required in climate modeling to ensure efficacy in hydrological applications. They noted that even models with partial accuracy (ratios above 0.5) are useful in predicting trends and variability, which are critical for water resource planning. In a related study, [63] also showed that gauge-based datasets should be preferred in regions with good weather network density, but satellite products would be good alternatives in data-sparse regions. In the same vein, regions with no or scarce observations, CPs can provide a viable alternative to hydrological simulations[2, 6, 64].

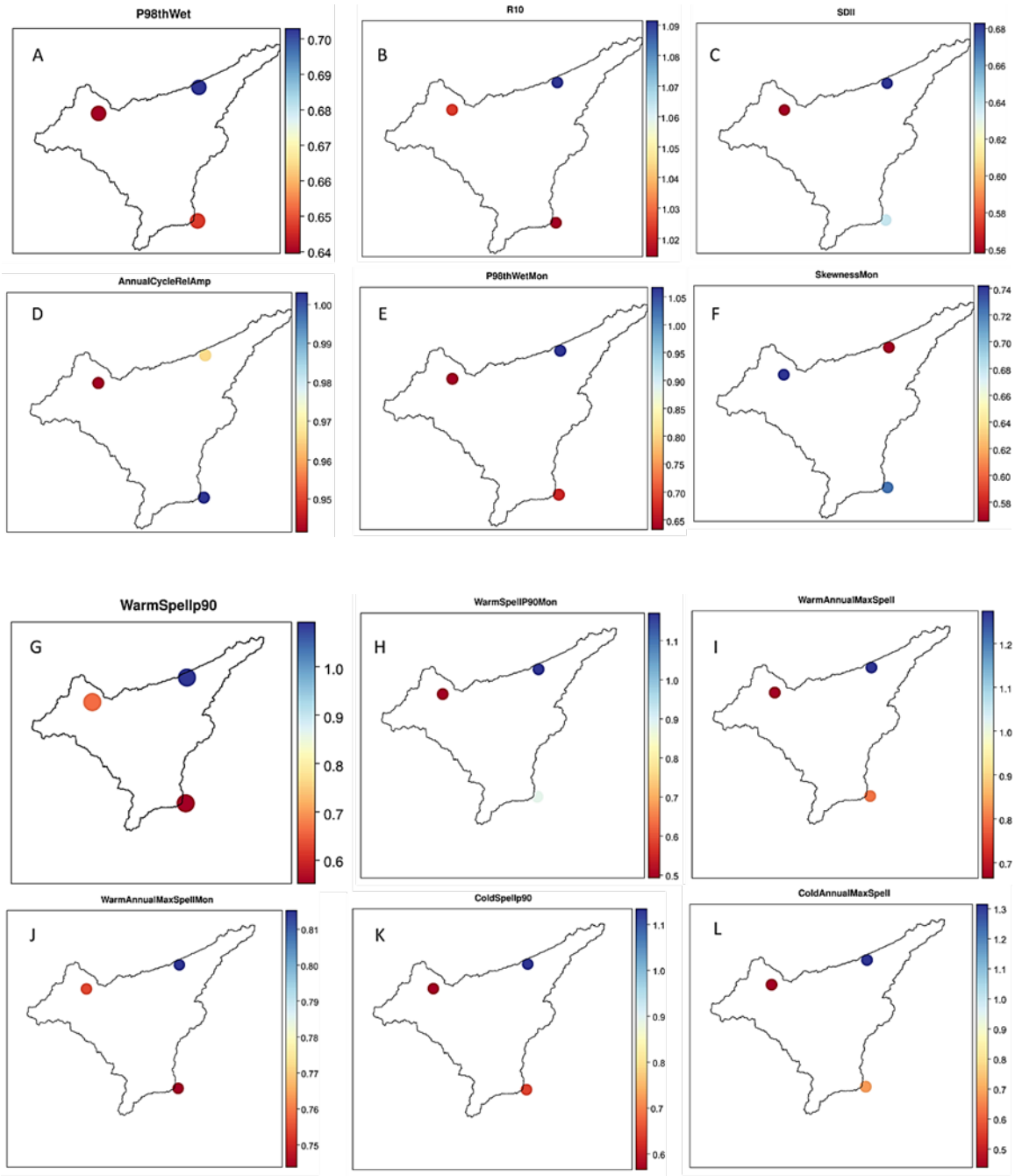

Received: 28/06/2025; Revised: 03/07/2025; Accepted: 03/07/2025; Published: 08/08/2025

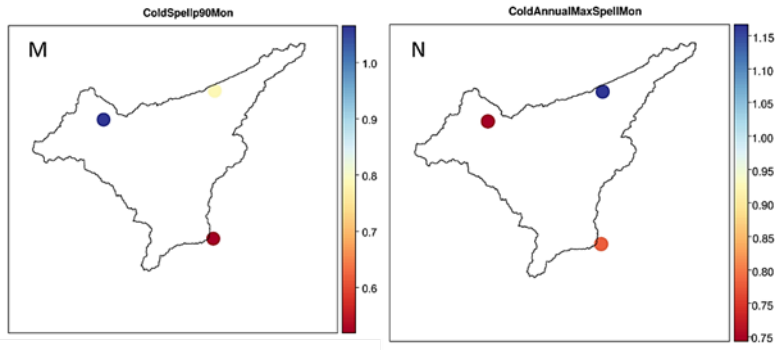

Figure 4: Extreme Ratios Pr (A, B, C, D, and F), Tmax (G, H, I, and J), and Tmin (K, L, M and N) for Daily and Monthly Extremes. The Monthly Indices are Attached with "Mon"

Bootstrapped uncertainty modelling of selected climate products

The bootstrapping uncertainty analysis, an integral component of this study, was conducted to assess the distributional fit and quantify the uncertainties associated with Tmax, Tmin, and Pr across the selected CPs within the HJRB. Table 6 presents the KS statistics for each distributional fit, with lower KS values indicating a better alignment between the fitted distribution and the data. The KS statistics serve as a quantitative measure of the goodness-of-fit, guiding the selection of the most appropriate distribution for each climatic variable and station. The analysis revealed distinct distributional fits for Tmax, Tmin, and Pr, varying across the stations. The log-normal distribution was identified as the most representative for bootstrapped Tmax data across all stations. This suggests that the log-normal distribution adequately captures the variability and skewness inherent in the Tmax data. For Tmin, the gamma distribution provided the best fit for the Kano station. In contrast, Weibull's distribution was found to be the best fit for Tmin in both Jigawa and Bauchi stations, reflecting the specific statistical properties of Tmin data in these regions. The analysis for precipitation data showed that Weibull's distribution was the most suitable for Kano and Jigawa stations, whereas the log-normal distribution best fitted the Pr data in the Bauchi station.

Table 6: Kolmogorov-Simonov (KS) test results

Variable/Station	Distribution	KS score
Pr, Kano	Normal	0.08
	Log-Normal	0.10
	Gamma	1.0
	Weibull	0.06
Pr, Jigawa	Normal	0.12
	Log-Normal	0.11
	Gamma	1.0
	Weibull	0.10
Pr, Bauchi	Normal	0.12
	Log-Normal	0.10
	Gamma	1.0
	Weibull	0.11
Tmax, Kano	Normal	0.09
	Log-Normal	0.08
	Gamma	1.0
	Weibull	0.10
Tmax, Jigawa	Normal	0.09
	Log-Normal	0.07
	Gamma	1.0
	Weibull	0.10
Tmax, Bauchi	Normal	0.11
	Log-Normal	0.09
	Gamma	1.0
	Weibull	0.14
Tmin, Kano	Normal	0.17
	Log-Normal	0.19
	Gamma	0.15

Received: 28/06/2025; Revised: 03/07/2025; Accepted: 03/07/2025; Published: 08/08/2025

Variable/Station	Distribution	KS score
	Weibull	0.14
Tmin, Jigawa	Normal	0.16
	Log-Normal	0.18
	Gamma	0.15
	Weibull	0.13
Tmin, Bauchi	Normal	0.18
	Log-Normal	0.20
	Gamma	0.10
	Weibull	0.15

Utilizing the identified best-fit distributions, 95% confidence intervals were determined for each quantile value ranging from 10% to 90% in the cumulative probability axis (y-axis). The integration of these quantile lines facilitated the construction of comprehensive uncertainty bands, which encapsulate the range of potential outcomes with a specified level of confidence. Figure 5 illustrates the constructed 95% uncertainty bands based on the bootstrapped CDFs. The figure effectively demonstrates how the uncertainty bands, derived from the 1000 bootstrapped replicas, encompass the CDF of the original sample data.

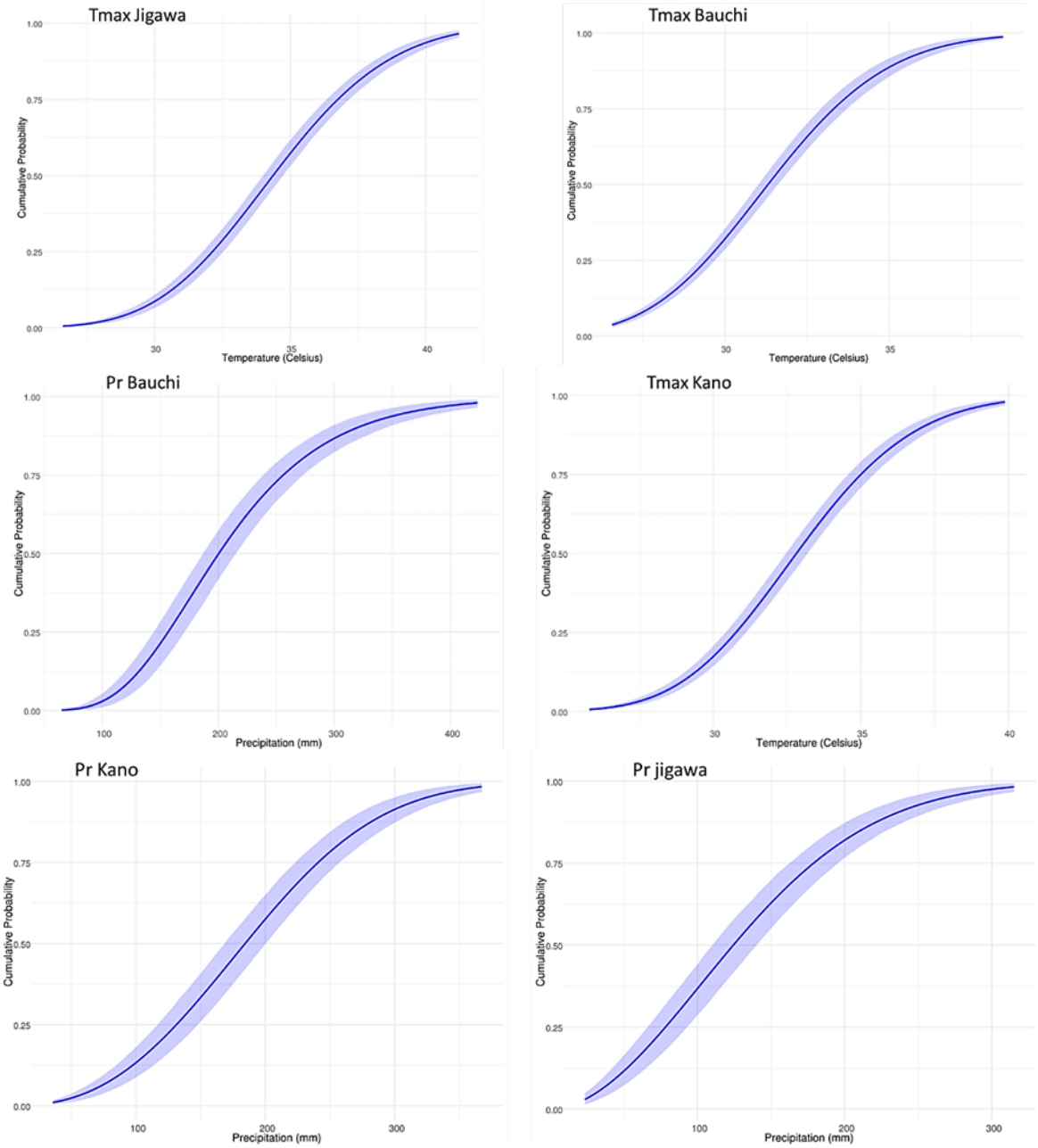

Received: 28/06/2025; Revised: 03/07/2025; Accepted: 03/07/2025; Published: 08/08/2025

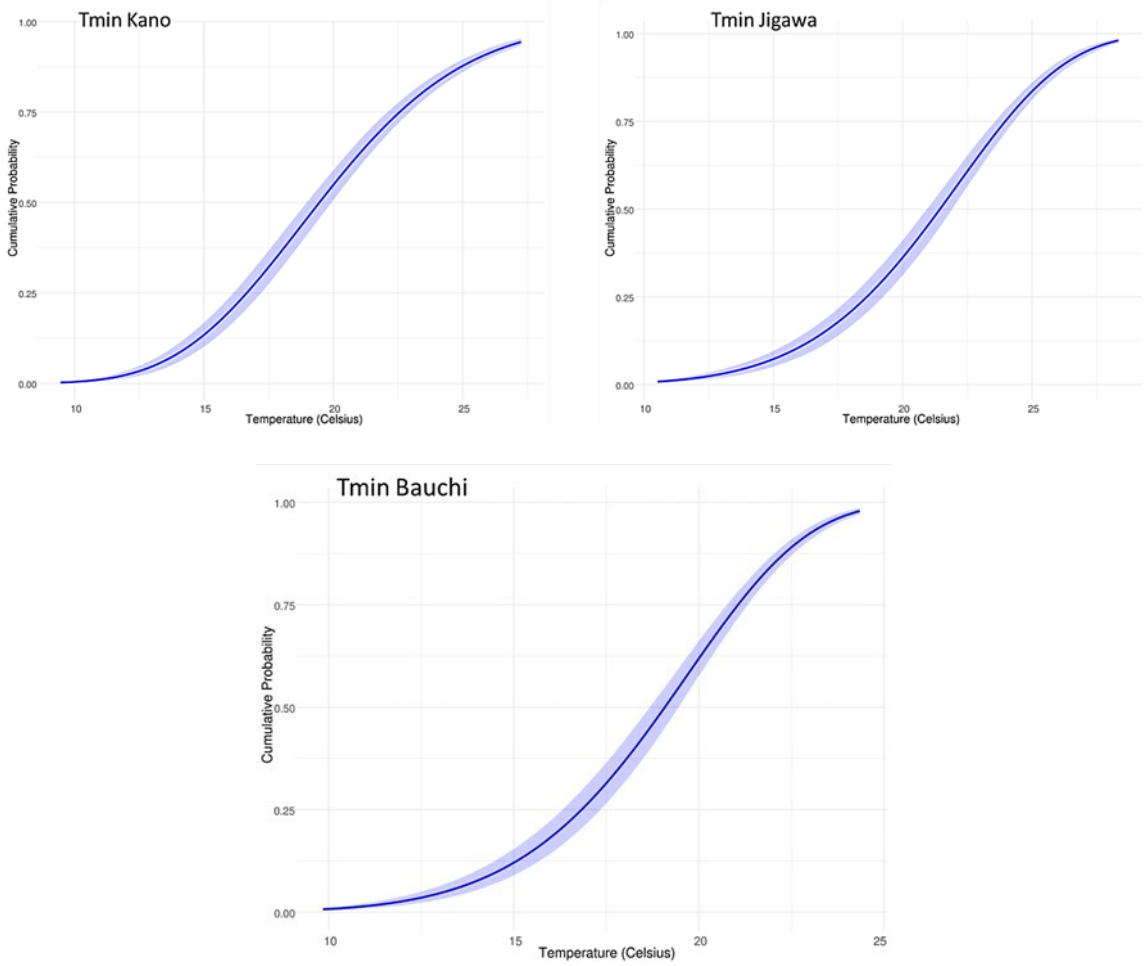

Figure 5: The Different Uncertainty Bands Obtained for each Station

In the bootstrapping uncertainty analysis, as shown in Figure 5, it's noteworthy that the constructed 95% uncertainty bands display a relatively narrow width. This characteristic of the uncertainty bands is particularly significant as it signifies a lower degree of uncertainty in the model predictions for Tmax, Tmin, and Pr across the stations. The narrow width of the uncertainty bands suggests that the bootstrapped replicas of the climate variables closely align with the original cumulative distribution function (CDF) of the raw data. This close alignment indicates that the variability within the 1000 bootstrapped replicas is limited, thereby pointing to a high level of confidence in the predictive accuracy of the selected distributions for Tmax, Tmin, and Pr. Such a finding is crucial for climate studies and applications within the basin, as it implies that the predictions made by the evaluated climate models, within the bounds of the identified distributions, are relatively precise. The lower uncertainty associated with these predictions enhances their reliability for various applications, including hydrological modeling, agricultural planning, and climate impact assessments.

4.0 Conclusion

This study presented an evaluation of climate models in the HJRB, employing a multifaceted approach that encompassed statistical metrics, Compromise Programming (CP), Multi-Criteria Group Decision Making (MCGDM). Furthermore, the selected product was subjected to climate extreme indices and bootstrapping uncertainty analysis. The aim was to rigorously assess the capability of various climate models in simulating key climatic variables; maximum temperature (Tmax), minimum temperature (Tmin), and precipitation (Pr) across the kano, Jigawa, and Bauchi stations within HJRB.

The performance of climate models was initially evaluated using a set of statistical metrics including NRMSE, MD, KGE, PBIAS, and r. These metrics were calculated at daily and monthly time steps to provide a detailed understanding of model performance.

CP was employed to combine the individual performance metrics into a single Compromise Programming Index (CPI), which facilitated a comparative analysis of model performances. The ERA5 model ranked as the top performer for Tmax and Tmin variables. CHIRPS was ranked best for precipitation patterns in the basin.

Received: 28/06/2025; Revised: 03/07/2025; Accepted: 03/07/2025; Published: 08/08/2025

The MCGDM approach synthesized model rankings across various stations to identify the most suitable models for the entire basin. Weights were assigned to models based on their rankings at each station, culminating in an integrated MCGDM index that guided the selection of the best models. ERA5 model was best for Tmax and Tmin, while CHIRPS stood out for Pr. Studies conducted by [63] showed that gauge-based datasets should be preferred in regions with good weather network density, however, CHIRPS and ERA5 would be good alternatives in data-sparse regions. In a similar study, CHIRPS and ERA5 products show good performance in tropical areas[7].

In the extreme indices calculation, the ratio of the climate products to the observation was taken. In all the extreme indices, the ratio exceeds 0.5, indicating an acceptable range for hydrological simulations[62]. For precipitation, the models are relatively accurate in simulating the seasonal variations as seen in the relative amplitude of the daily annual cycle. Hence their applicability in hydrological model simulation. The temperature indices from the analyses yielded an overall good performance.

The uncertainty associated with model predictions was quantified using bootstrapping techniques, which involved generating 1000 replicas of the data to evaluate the best-fit statistical distributions. The log-normal distribution was found to be most representative of Tmax across all stations, while the gamma and Weibull distributions best fitted Tmin and Pr data, respectively, depending on the station. The constructed 95% uncertainty bands, derived from the bootstrapped data, revealed a narrow width, indicating low uncertainty in the selected CPs.

Nonetheless, the study is constrained by the availability of only three meteorological stations with continuous, quality-checked data from 1990 to 2015. This limited spatial coverage may restrict the generalizability of the results across the entire basin. Incorporating a denser observational network would enhance the robustness of model validation. Additionally, future research should consider integrating standardized drought indices such as the Standardized Precipitation Index (SPI) to complement existing metrics and better assess the capability of climate products in capturing interannual variability and extreme climate events.

References

[1] M. Tarek, F. P. Brissette, and R. Arsenault, "Evaluation of the ERA5 reanalysis as a potential reference dataset for hydrological modelling over North America," *Hydrology and Earth System Sciences,* vol. 24, no. 5, pp. 2527-2544, 2020.

[2] A. J. Koutsouris, D. Chen, and S. W. Lyon, "Comparing global precipitation data sets in eastern Africa: a case study of Kilombero Valley, Tanzania," *International Journal of Climatology,* vol. 36, no. 4, pp. 2000-2014, 2015.

[3] M. T. Z. Ahmad, *Assessment of Sustainable Efficiency (Sefficiency) and Water Allocation Under Uncertainty in Kano River Basin*. 2018.

[4] C. Li, T. Zhao, C. Shi *et al.*, "Evaluation of Daily Precipitation Product in China from the CMA Global Atmospheric Interim Reanalysis," *Journal of Meteorological Research,* vol. 34, no. 1, pp. 117-136, 2020/02/01 2020.

[5] N. Wang, W. Liu, F. Sun *et al.*, "Evaluating satellite-based and reanalysis precipitation datasets with gauge-observed data and hydrological modeling in the Xihe River Basin, China," *Atmospheric Research,* vol. 234, p. 104746, 2020/04/01/ 2020.

[6] J. Peng, T. Liu, Y. Huang *et al.*, "Satellite-Based Precipitation Datasets Evaluation Using Gauge Observation and Hydrological Modeling in a Typical Arid Land Watershed of Central Asia," *Remote Sensing,* vol. 13, no. 2, 2021.

[7] A. H. Al-Falahi, N. Saddique, U. Spank *et al.*, "Evaluation the Performance of Several Gridded Precipitation Products over the Highland Region of Yemen for Water Resources Management," *Remote Sensing,* vol. 12, no. 18, 2020.

[8] Y. Zhang and N. Ma, "Spatiotemporal variability of snow cover and snow water equivalent in the last three decades over Eurasia," *Journal of Hydrology,* vol. 559, pp. 238-251, 2018/04/01/ 2018.

[9] T. Dinku, P. Ceccato, E. Grover-Kopec *et al.*, "Validation of satellite rainfall products over East Africa's complex topography," *International Journal of Remote Sensing,* vol. 28, no. 7, pp. 1503-1526, 2007.

[10] T. C. Liechti, J. P. Matos, J. L. Boillat *et al.*, "Comparison and evaluation of satellite derived precipitation products for hydrological modeling of the Zambezi River Basin," *Hydrology and Earth System Sciences,* vol. 16, no. 2, pp. 489-500, 2012.

[11] R. Maidment, D. I. F. Grimes, R. P. Allan *et al.*, "Evaluation of satellite-based and model re-analysis rainfall estimates for Uganda," *Meteorological Applications,* vol. 20, no. 3, pp. 308-317, 2012.

[12] F. Mashingia, F. Mtalo, and M. Bruen, "Validation of Remotely Sensed Rainfall over Major Climatic Regions in Northeast Tanzania," *Physics and Chemistry of the Earth, Parts A/B/C,* vol. 67, no. NA, pp. 55-63, 2014.

Received: 28/06/2025; Revised: 03/07/2025; Accepted: 03/07/2025; Published: 08/08/2025

[13] T. G. Romilly and M. Gebremichael, "Evaluation of satellite rainfall estimates over Ethiopian river basins," *Hydrology and Earth System Sciences,* vol. 15, no. 5, pp. 1505-1514, 2011.
[14] E. Habib, M. ElSaadani, and A. T. Haile, "Climatology-Focused Evaluation of CMORPH and TMPA Satellite Rainfall Products over the Nile Basin," *Journal of Applied Meteorology and Climatology,* vol. 51, no. 12, pp. 2105-2121, 2012.
[15] Q. Zhang, H. Körnich, and K. Holmgren, "How well do reanalyses represent the southern African precipitation," *Climate Dynamics,* vol. 40, no. 3, pp. 951-962, 2012.
[16] M. Alijanian, G. R. Rakhshandehroo, A. K. Mishra *et al.*, "Evaluation of satellite rainfall climatology using CMORPH, PERSIANN-CDR, PERSIANN, TRMM, MSWEP over Iran," *International Journal of Climatology,* vol. 37, no. 14, pp. 4896-4914, 2017.
[17] D. C. Buarque, R. C. D. de Paiva, R. T. Clarke *et al.*, "A comparison of Amazon rainfall characteristics derived from TRMM, CMORPH and the Brazilian national rain gauge network," *Journal of Geophysical Research,* vol. 116, no. D19, pp. NA-NA, 2011.
[18] K. Bumke, G. König-Langlo, J. Kinzel *et al.*, "HOAPS and ERA-Interim precipitation over the sea: validation against shipboard in situ measurements," *Atmospheric Measurement Techniques,* vol. 9, no. 5, pp. 2409-2423, 2016.
[19] F. A. Hirpa, M. Gebremichael, and T. Hopson, "Evaluation of High-Resolution Satellite Precipitation Products over Very Complex Terrain in Ethiopia," *Journal of Applied Meteorology and Climatology,* vol. 49, no. 5, pp. 1044-1051, 2010.
[20] A. AghaKouchak, A. Behrangi, S. Sorooshian *et al.*, "Evaluation of satellite-retrieved extreme precipitation rates across the central United States," *Journal of Geophysical Research,* vol. 116, no. D2, pp. NA-NA, 2011.
[21] T. Islam, M. A. Rico-Ramirez, D. Han *et al.*, "Performance Evaluation of the TRMM Precipitation Estimation Using Ground-Based Radars from the GPM Validation Network," *Journal of Atmospheric and Solar-Terrestrial Physics,* vol. 77, no. NA, pp. 194-208, 2012.
[22] A. Behrangi, B. Khakbaz, T. C. Jaw *et al.*, "Hydrologic evaluation of satellite precipitation products over a mid-size basin," *Journal of Hydrology,* vol. 397, no. 3, pp. 225-237, 2011.
[23] M. M. Bitew, M. Gebremichael, L. T. Ghebremichael *et al.*, "Evaluation of High-Resolution Satellite Rainfall Products through Streamflow Simulation in a Hydrological Modeling of a Small Mountainous Watershed in Ethiopia," *Journal of Hydrometeorology,* vol. 13, no. 1, pp. 338-350, 2012.
[24] B. Collischonn, W. Collischonn, and C. E. M. Tucci, "Daily hydrological modeling in the Amazon basin using TRMM rainfall estimates," *Journal of Hydrology,* vol. 360, no. 1, pp. 207-216, 2008.
[25] A. S. Falck, V. Maggioni, J. Tomasella *et al.*, "Propagation of satellite precipitation uncertainties through a distributed hydrologic model: A case study in the Tocantins–Araguaia basin in Brazil," *Journal of Hydrology,* vol. 527, no. NA, pp. 943-957, 2015.
[26] C. Albergel, W. Dorigo, R. H. Reichle *et al.*, "Skill and Global Trend Analysis of Soil Moisture from Reanalyses and Microwave Remote Sensing," *Journal of Hydrometeorology,* vol. 14, no. 4, pp. 1259-1277, 2013.
[27] B. Martens, D. G. Miralles, H. Lievens *et al.*, "GLEAM v3: satellite-based land evaporation and root-zone soil moisture," *Geoscientific Model Development,* vol. 10, no. 5, pp. 1903-1925, 2017.
[28] M. Pan, H. Li, and E. F. Wood, "Assessing the skill of satellite-based precipitation estimates in hydrologic applications," *Water Resources Research,* vol. 46, no. 9, pp. NA-NA, 2010.
[29] W. Dong, G. Wang, L. Guo *et al.*, "Evaluation of Three Gridded Precipitation Products in Characterizing Extreme Precipitation over the Hengduan Mountains Region in China," *Remote Sensing,* vol. 14, no. 17, p. 4408, 2022.
[30] S. H. Gebrechorkos, S. Hülsmann, and C. Bernhofer, "Evaluation of multiple climate data sources for managing environmental resources in East Africa," *Hydrology and Earth System Sciences,* vol. 22, no. 8, pp. 4547-4564, 2018.
[31] M. S. Nashwan, S. Shahid, and X. Wang, "Assessment of satellite-based precipitation measurement products over the hot desert climate of Egypt," *Remote Sensing,* vol. 11, no. 5, pp. 555-NA, 2019.
[32] R. Saeidizand, S. Sabetghadam, E. Tarnavsky *et al.*, "Evaluation of CHIRPS rainfall estimates over Iran," *Quarterly Journal of the Royal Meteorological Society,* vol. 144, no. S1, pp. 282-291, 2018.
[33] J. Fang, W. Yang, Y. Luan *et al.*, "Evaluation of the TRMM 3B42 and GPM IMERG products for extreme precipitation analysis over China," *Atmospheric Research,* vol. 223, no. NA, pp. 24-38, 2019.
[34] D. Li, G. Christakos, X. Ding *et al.*, "Adequacy of TRMM satellite rainfall data in driving the SWAT modeling of Tiaoxi catchment (Taihu lake basin, China)," *Journal of Hydrology,* vol. 556, no. NA, pp. 1139-1152, 2018.
[35] A. J. Khan, M. Koch, and K. M. Chinchilla, "Evaluation of Gridded Multi-Satellite Precipitation Estimation (TRMM-3B42-V7) Performance in the Upper Indus Basin (UIB)," *Climate,* vol. 6, no. 3, pp. 76-NA, 2018.

Received: 28/06/2025; Revised: 03/07/2025; Accepted: 03/07/2025; Published: 08/08/2025

[36] H. Ashouri, K. Hsu, S. Sorooshian *et al.*, "PERSIANN-CDR: Daily Precipitation Climate Data Record from Multisatellite Observations for Hydrological and Climate Studies," *Bulletin of the American Meteorological Society,* vol. 96, no. 1, pp. 69-83, 2015.

[37] K. M. Bâ, L. Balcázar, V. Diaz *et al.*, "Hydrological Evaluation of PERSIANN-CDR Rainfall over Upper Senegal River and Bani River Basins," *Remote Sensing,* vol. 10, no. 12, pp. 1884-NA, 2018.

[38] S. T. Ogunjo, C. F. Olusegun, and I. A. Fuwape, "Evaluation of Monthly Precipitation Data from Three Gridded Climate Data Products over Nigeria," *Remote Sensing in Earth Systems Sciences,* vol. 5, no. 3, pp. 119-128, 2022/09/01 2022.

[39] A. A. Salami, J. F. Olorunfemi, and A. O. Eludoyin, "Multi-Criteria Assessment of Gridded Rainfall Data Accuracy in Nigeria Using Compromise Programming," *Earth Systems and Environment,* 2025/02/14 2025.

[40] B. Tanimu, M. M. Hamed, A.-A. D. Bello *et al.*, "Selecting the optimal gridded climate dataset for Nigeria using advanced time series similarity algorithms," *Environmental Science and Pollution Research,* vol. 31, no. 10, pp. 15986-16010, 2024/02/01 2024.

[41] K. N. Ogbu, N. R. Hounguè, I. E. Gbode *et al.*, "Performance Evaluation of Satellite-Based Rainfall Products over Nigeria," *Climate,* vol. 8, no. 10, p. 103, 2020.

[42] H. Hersbach, B. Bell, P. Berrisford *et al.*, "The ERA5 global reanalysis," *Quarterly Journal of the Royal Meteorological Society,* vol. 146, no. 730, pp. 1999-2049, 2020.

[43] R. Gelaro, W. McCarty, M. J. Suárez *et al.*, "The modern-era retrospective analysis for research and applications, version 2 (MERRA-2)," *Journal of climate,* vol. 30, no. 14, pp. 5419-5454, 2017.

[44] S. Saha, S. Moorthi, H.-L. Pan *et al.*, "The NCEP climate forecast system reanalysis," *Bulletin of the American Meteorological Society,* vol. 91, no. 8, pp. 1015-1058, 2010.

[45] C. Funk, P. Peterson, M. Landsfeld *et al.*, "The climate hazards infrared precipitation with stations--a new environmental record for monitoring extremes," *Scientific data,* vol. 2, no. 1, pp. 150066-150066, 2015.

[46] U. Schneider, T. Fuchs, A. Meyer-Christoffer *et al.*, "Global precipitation analysis products of the GPCC," *Global Precipitation Climatology Centre (GPCC), DWD, Internet Publikation,* vol. 112, 2008.

[47] B. Rudolf, A. Becker, U. Schneider *et al.*, "The new "GPCC Full Data Reanalysis Version 5" providing high-quality gridded monthly precipitation data for the global land-surface is public available since December 2010," *GPCC Status rep,* vol. 7, 2010.

[48] M. Chen, W. Shi, P. Xie *et al.*, "Assessing objective techniques for gauge-based analyses of global daily precipitation," *Journal of Geophysical Research: Atmospheres,* vol. 113, no. D4, 2008.

[49] D. K. Braithwaite, S. Sorooshian, K.-L. Hsu *et al.*, "PERSIANN-CDR: Daily Precipitation Climate Data Record from Multisatellite Observations for Hydrological and Climate Studies," *Bulletin of the American Meteorological Society,* vol. 96, no. 1, pp. 69-83, 2015.

[50] C. Funk, P. Peterson, M. Landsfeld *et al.*, "The climate hazards infrared precipitation with stations--a new environmental record for monitoring extremes," *Sci Data,* vol. 2, p. 150066, Dec 8 2015.

[51] H. Hersbach, B. Bell, P. Berrisford *et al.*, "The ERA5 global reanalysis," *Quarterly Journal of the Royal Meteorological Society,* vol. 146, no. 730, pp. 1999-2049, 2020.

[52] R. Gelaro, W. McCarty, M. J. Suarez *et al.*, "The Modern-Era Retrospective Analysis for Research and Applications, Version 2 (MERRA-2)," *J Clim,* vol. Volume 30, no. Iss 13, pp. 5419-5454, Jun 20 2017.

[53] S. Saha, S. Moorthi, H.-L. Pan *et al.*, "The NCEP Climate Forecast System Reanalysis," *Bulletin of the American Meteorological Society,* vol. 91, no. 8, pp. 1015-1058, 2010.

[54] S. Bhattacharyya, S. Sreekesh, and A. King, "Characteristics of extreme rainfall in different gridded datasets over India during 1983–2015," *Atmospheric Research,* vol. 267, 2022.

[55] M. Iturbide, J. Bedia, S. Herrera *et al.*, "The R-based climate4R open framework for reproducible climate data access and post-processing," *Environmental Modelling & Software,* vol. 111, pp. 42-54, 2019/01/01/ 2019.

[56] J. Bedia, J. Baño-Medina, M. N. Legasa *et al.*, "Statistical downscaling with the downscaleR package (v3.1.0): contribution to the VALUE intercomparison experiment," *Geoscientific Model Development,* vol. 13, no. 3, pp. 1711-1735, 2020.

[57] H. Galavi, M. Mirzaei, B. Yu *et al.*, "Bootstrapped ensemble and reliability ensemble averaging approaches for integrated uncertainty analysis of streamflow projections," *Stochastic Environmental Research and Risk Assessment,* vol. 37, no. 4, pp. 1213-1227, 2022.

[58] B. Efron, "Bootstrap methods: another look at the jackknife," in *Breakthroughs in statistics: Methodology and distribution*: Springer, 1992, pp. 569-593.

[59] A. D. Datti, G. Zeng, E. Tarnavsky *et al.*, "Evaluation of Satellite-Based Rainfall Estimates against Rain Gauge Observations across Agro-Climatic Zones of Nigeria, West Africa," *Remote Sensing,* vol. 16, no. 10, p. 1755, 2024.

[60] S. H. Gebrechorkos, J. Leyland, S. J. Dadson *et al.*, "Global-scale evaluation of precipitation datasets for hydrological modelling," *Hydrol. Earth Syst. Sci.,* vol. 28, no. 14, pp. 3099-3118, 2024.

Received: 28/06/2025; Revised: 03/07/2025; Accepted: 03/07/2025; Published: 08/08/2025

[61] C. Kouakou, J.-E. Paturel, F. Satgé *et al.*, "Comparison of gridded precipitation estimates for regional hydrological modeling in West and Central Africa," *Journal of Hydrology: Regional Studies,* vol. 47, p. 101409, 2023/06/01/ 2023.

[62] F. H. S. Chiew and T. A. McMahon, "Modelling the impacts of climate change on Australian streamflow," *Hydrological Processes,* vol. 16, no. 6, pp. 1235-1245, 2002.

[63] M. Tarek, F. P. Brissette, and R. Arsenault, "Large-Scale Analysis of Global Gridded Precipitation and Temperature Datasets for Climate Change Impact Studies," *Journal of Hydrometeorology,* vol. 21, no. 11, pp. 2623-2640, 2020.

[64] S. Bhattacharyya, S. Sreekesh, and A. King, "Characteristics of extreme rainfall in different gridded datasets over India during 1983–2015," *Atmospheric Research,* vol. 267, p. 105930, 2022/04/01/ 2022.

Received: 28/06/2025; Revised: 03/07/2025; Accepted: 03/07/2025; Published: 08/08/2025